PHYSICAL REVIEW B VOLUME 56, NUMBER 24 15 DECEMBER 1997-II

Enhanced anti-Stokes photoluminescence in a GaAs/$Al_{0.17}Ga_{0.83}As$ single quantum well with growth islands

L. Schrottke and H. T. Grahn
Paul-Drude-Institut für Festkörperelektronik, Hausvogteiplatz 5-7, D-10117 Berlin, Germany

K. Fujiwara
Department of Electrical Engineering, Kyushu Institute of Technology, Tobata, Kitakyushu 804, Japan
(Received 23 September 1997)

Photoluminescence spectra of a GaAs/$Al_{0.17}Ga_{0.83}As$ single quantum well with growth islands are investigated in the Stokes as well as in the anti-Stokes regime. While at 5 K only luminescence at energies below the excitation energy can be detected, above 20 K also anti-Stokes luminescence is observed. A rate-equation model reproduces the observed dependence of the intensities of Stokes and anti-Stokes luminescence on temperature and, qualitatively, on the areal density of the growth islands and the properties of the diffusion-assisted transfer between them. The geometrical properties can enhance the anti-Stokes luminescence by almost one order of magnitude. [S0163-1829(97)51548-7]

The optical and dynamical properties of excitons in semiconductor quantum wells (QW's) have been of great interest for the last decade. Molecular-beam epitaxy allows the fabrication of high-quality QW structures, e.g., GaAs/$Al_xGa_{1-x}As$ QW's (Ref. 1) or InAs/InP QW's,[2] with atomically flat terraces larger than the exciton Bohr radius. In such samples, the perturbations of the potential for the quantum confinement, which results from statistical variations of the well width and/or of the alloy composition, may be separated into macroroughness (correlation lengths $>$exciton Bohr radius) and microroughness (correlation length$<$exciton Bohr radius). While macroroughness leads to multiple lines in the photoluminescence (PL) spectra with an energy separation of the excitonic states of several meV, microroughness provides many localized excitonic states, into which the excitons may quickly relax.

The H_1E_1 excitons (ground state of the heavy-hole band with the conduction-band ground state) can be created either by energy relaxation of electron-hole pairs excited well above this transition or by resonant excitation. Since the formation time of excitons is much faster than any transfer time of the excitons between growth islands, a quantitative analysis can be restricted to the kinetics of the exciton population on the basis of a rate equation model.[1,3] Applying such a model to QW structures with growth islands, usually the rates for generation and recombination of excitons, the exciton trapping time within each QW, and the transfer time from one QW island to the adjacent one are taken into account. In contrast to the transition to wider-well islands, i.e., the energy relaxation of the excitons via emission of acoustical phonons, the transition to narrower-well islands, i.e., the activation via absorption of acoustical phonons, depends strongly on temperature.[4] While at low temperatures (5 K) activation processes may be neglected since the thermal energy (approximately 1 meV) is too small, they reach a finite probability for higher temperatures. In this situation, the thermal energy is larger than the potential step between adjacent islands so that also exciton states with higher energy become significantly populated due to heating of cold excitons (cf. also Ref. 5).

In the case of resonant excitation into a single growth island, the population of energetically higher states in neighboring islands leads to the observation of luminescence at higher energies than the excitation energy, which is referred to as anti-Stokes PL. In contrast to several other processes, which can lead to anti-Stokes PL in semiconductor samples, such as two-step excitation involving deep level states,[6–8] quantum oscillations in a GaAs/$Al_xGa_{1-x}As$ asymmetric double QW,[9] or impact activation of excitons by hot electrons (GaAs/$Al_xGa_{1-x}As$ multiple QW structures),[10] the anti-Stokes luminescence described in this paper for a single QW exhibits a significant dependence on the geometrical properties of the growth islands such as their areal density. The importance of the geometry is discussed within the framework of a kinetic model for the excitons. The theoretical estimation is compared with the experimental results, which shows that the anti-Stokes luminescence of some of the growth islands is considerably enhanced.

A 5.5-nm-wide GaAs/$Al_{0.17}Ga_{0.83}As$ QW was grown by molecular-beam epitaxy using 2 min growth interruption at the GaAs well interfaces. For the PL experiments, the sample was mounted in a He-flow cryostat. The optical excitation was carried out with a tunable Ti:sapphire laser pumped by an Ar^+ laser. The PL signal was dispersed in a 1 m monochromator and detected with a cooled charge-coupled-device detector. The laser power was adjusted to 0.2 μW with the beam focused to a diameter of about 50 μm. We previously performed a very detailed investigation of the PL spectra of this sample as a function of excitation energy with high resolution, which we refer to as high-resolution PLE.[11]

In Figs. 1(a)–1(c) the PL intensities measured at 5, 20, and 40 K, respectively, are shown as a function of both the excitation and the detection energy using a grayscale representation. A horizontal cut in this graph corresponds to a single PL spectrum, a vertical cut to a single PLE spectrum. The data were recorded as PL spectra as a function of excitation energy using 1 meV steps. In this representation, the splitting of the PL lines due to monolayer islands appears as five narrow, parallel lines in the vertical direction. The two

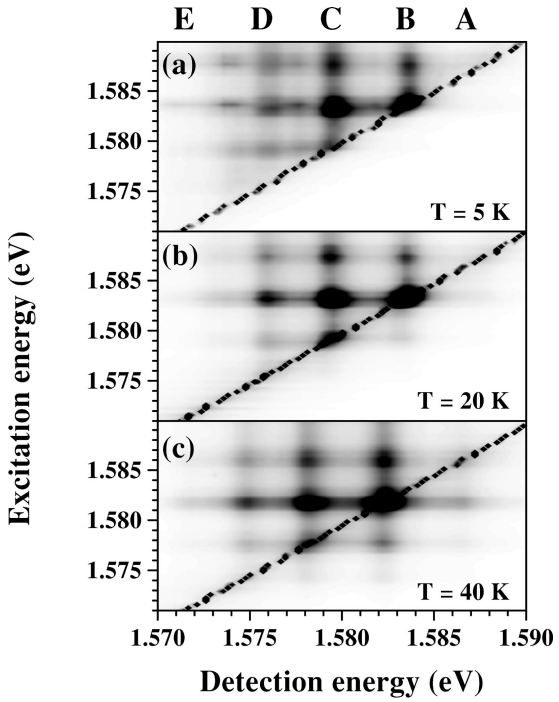

FIG. 1. PL intensity of a 5.5-nm-wide QW as a function of detection as well as excitation energy at (a) 5, (b) 20, and (c) 40 K. The PL spectra exhibit PL maxima for 5 monolayer islands $A-E$ (marked on top). The images are divided by the laser energy (dotted line) into the Stokes region, i.e., where $E_{\mathrm{det}}<E_{\mathrm{exc}}$ (upper-left part), and the anti-Stokes region, i.e., $E_{\mathrm{det}}>E_{\mathrm{exc}}$ (lower-right part).

additional lines, which appear 2 meV below the lines of islands C and D, are attributed to bound excitons (cf. Ref. 11). At excitation energies corresponding to the PL energies of the QW's, the holes from the first heavy-hole subband are directly excited into the first conduction subband resulting in pronounced maxima of the PL intensity, which appear as horizontal lines.

The stray light of the laser, which produces a broad (dashed) line for the condition detection energy=excitation energy, is also shown in the grayscale representation. This line separates the region of the Stokes luminescence (upper left part) from the region of the anti-Stokes luminescence (lower right part). At 5 K no anti-Stokes luminescence is observed, while already at 20 K a significant luminescence intensity is indicated close to the laser line for detection energies larger than the excitation energy. Finally, at 40 K the anti-Stokes luminescence is very intense and is present also in growth islands with well thicknesses differing by more than one monolayer from the resonantly excited well. In addition to the increasing intensity of the anti-Stokes luminescence, a shift of the peak positions to lower energies can be observed with increasing temperature, e.g., the PL maximum of island C shifts from 1.5795 eV (at 5 K) to 1.578 eV (at 40 K). Figure 2 shows the PL spectra for resonant excitation into island C at 20 and 40 K. At these temperatures, the ratios of anti-Stokes and Stokes luminescence, which are obtained by integrating the intensities of the respective PL lines, are about 0.4 and 2.1, respectively.

For a quantitative analysis, a system of rate equations is used similar to the model described in Ref. 1. However, since only the stationary state is of interest, the exciton trapping time within the islands is neglected, so that we do not distinguish between free and bound excitons. Furthermore, also transfer processes from wider to narrower QW's have to be considered, i.e., a thermal activation of excitons from energetically lower to higher states is allowed. With N_i denoting the exciton densities as well as g_i the generation rates in the ith growth island, τ_{ij} the transition times from the ith to the jth island $(i,j=A,B,C,D,E)$, and τ_r the recombination time, which is assumed to be the same for each island, the rate-equation model reads as follows:

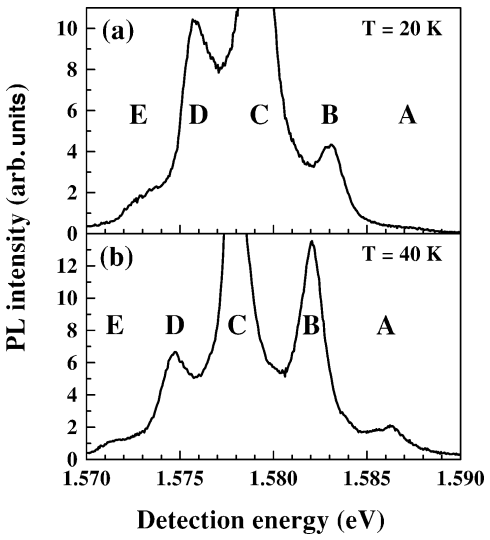

FIG. 2. PL spectra for resonant excitation into island C at (a) 20 and (b) 40 K. The integrated intensity ratio of peaks B and D has a value of about 0.4 and 2.1 at 20 and 40 K, respectively.

$$\frac{dN_A}{dt}=g_A-\frac{N_A}{\tau_r}-\frac{N_A}{\tau_{AB}}+\frac{N_B}{\tau_{BA}}, \tag{1}$$

$$\frac{dN_B}{dt}=g_B-\frac{N_B}{\tau_r}-\frac{N_B}{\tau_{BC}}-\frac{N_B}{\tau_{BA}}+\frac{N_C}{\tau_{CB}}+\frac{N_A}{\tau_{AB}}, \tag{2}$$

$$\frac{dN_C}{dt}=g_C-\frac{N_C}{\tau_r}-\frac{N_C}{\tau_{CD}}-\frac{N_C}{\tau_{CB}}+\frac{N_D}{\tau_{DC}}+\frac{N_B}{\tau_{BC}}, \tag{3}$$

$$\frac{dN_D}{dt}=g_D-\frac{N_D}{\tau_r}-\frac{N_D}{\tau_{DE}}-\frac{N_D}{\tau_{DC}}+\frac{N_E}{\tau_{ED}}+\frac{N_C}{\tau_{CD}}, \tag{4}$$

$$\frac{dN_E}{dt}=g_E-\frac{N_E}{\tau_r}-\frac{N_E}{\tau_{ED}}+\frac{N_D}{\tau_{DE}}. \tag{5}$$

For Eqs. (1)–(5), only nearest-neighbor transitions are taken into account. In contrast to Ref. 1, where the excitation energy is well above the ground states of the QW and, consequently, the generation rate in each island is assumed to be proportional to the areal density, we assume a strictly resonant excitation, i.e., the exciting laser is well tuned to the H_1E_1 transition of precisely one island. Consequently, all generation rates g_i but one are zero. In the stationary state,

the time derivatives must be zero so that Eqs. (1)–(5) evolve into an inhomogeneous system of linear equations, which can be solved analytically.

In order to estimate the significance of the anti-Stokes PL, we have quantitatively analyzed the ratio of the PL intensities of island B and D, ρ_{BD}, at resonant excitation into island C. In this configuration, an exciton density is provided that is sufficient for the detection of the PL from both islands B and D at 20 K as well as at 40 K (cf. Fig. 2). The PL intensity of the ith island is proportional to its areal density a_i, i.e., $I_i = a_i N_i / \tau_r$. Since the PL intensities of islands A and E are very low, we will neglect the exciton densities for these two islands. The ratio ρ_{BD} is then given by

$$\rho_{BD} = \frac{I_B}{I_D} = \frac{a_B}{a_D}\frac{N_B}{N_D} = \frac{a_B}{a_D}\frac{\tau_{CD}\tau_{BC}(\tau_{DC}+\tau_r)}{\tau_{CB}\tau_{DC}(\tau_{BC}+\tau_r)}. \tag{6}$$

The transition times τ_{ij}, i.e., the reciprocal of the transition probabilities, can be split into a phonon factor τ_{ij}^{ϕ}, which describes the energy transfer due to emission and absorption of acoustical phonons, and a diffusion factor γ_{ij}, which depends on size and distribution of the islands as well as the properties of the diffusion-assisted transfer between islands, $\tau_{ij} = \tau_{ij}^{\phi}\gamma_{ij}$. Since τ_{ij}^{ϕ} depends only on temperature and the energy difference between the states of adjacent wells, which is approximately the same for all islands, τ_- denotes the relaxation while τ_+ refers to the activation processes. Using the Bose-Einstein distribution, with ΔE denoting the energy separation of the monolayer splitting and k_B Boltzmann's constant, we obtain for phonon emission

$$\tau_- = \tau_0(1 - e^{-\Delta E/k_B T}) \tag{7}$$

and for phonon absorption

$$\tau_+ = \tau_0(e^{\Delta E/k_B T} - 1) \tag{8}$$

(cf., e.g., Ref. 12). Finally, the ratio ρ_{BD} is

$$\rho_{BD} = \frac{a_B}{a_D}\frac{\gamma_{CD}\gamma_{BC}}{\gamma_{CB}\gamma_{DC}}\frac{\tau_-^2}{\tau_+^2}\frac{(\gamma_{DC}\tau_+ + \tau_r)}{(\gamma_{BC}\tau_- + \tau_r)}. \tag{9}$$

This ratio depends on the radiative properties of the system via τ_r, on temperature and the energy distance between the excitonic states in the wells via τ_+ and τ_-, and, in a more complex way, on the diffusion-assisted transfer as well as the geometry via γ_{ij} and a_i.

In an idealized three-level system without any spatial geometry of the excitonic states, for which their occupation would only depend on the thermal activation by interaction with acoustical phonons, the geometry factors are the same for each transition, i.e., $\gamma_{ij} = \gamma_0$ and $a_i = a_0$. In this case, the ratio between the anti-Stokes and the Stokes luminescence is

$$\rho_{BD} = \frac{\tau_-^2(\tau_+\gamma_0 + \tau_r)}{\tau_+^2(\tau_-\gamma_0 + \tau_r)}. \tag{10}$$

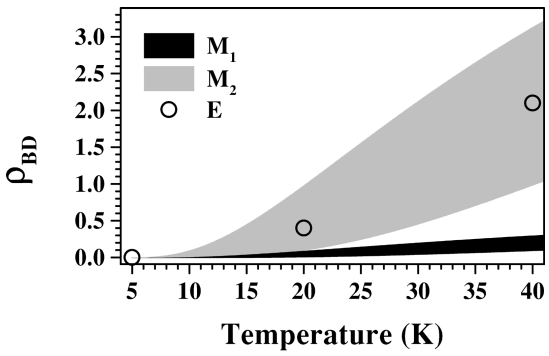

FIG. 3. M_1: possible values for ρ_{BD} according to Eq. (11), M_2: possible values for ρ_{BD} taking into account the areal densities a_B and a_D, and E: the experimental results for ρ_{BD} as a function of the temperature.

Unfortunately, neither γ_0 nor τ_r are sufficiently well known for a calculation of ρ_{BD}. However, with $\tau_- < \tau_+$ (which is obviously true), the inequality

$$\frac{\tau_-^2}{\tau_+^2} < \rho_{BD} < \frac{\tau_-}{\tau_+} \tag{11}$$

can be derived. For $\Delta E = 4$ meV, we obtain at 20 and 40 K $0.01 < \rho_{BD}(20\text{ K}) < 0.1$ and $0.1 < \rho_{BD}(40\text{ K}) < 0.31$, respectively.

In Fig. 3, the black area M_1 shows the possible values for ρ_{BD} according to the above-described theoretical estimation as a function of temperature. The comparison with the experimental results of ρ_{BD} indicated by the circles E shows that they are almost one order of magnitude larger than the estimated values. Therefore, the areal densities, which play an important role for ρ_{BD} according to Eq. (9), have to be considered. The areal densities of the islands were estimated using integrated PLE spectra, i.e., the total luminescence intensity integrated over all growth islands as a function of the excitation energy. We determined the following values: $a_A \approx 0.3$, $a_B \approx 0.5$, $a_C \approx 0.14$, $a_D \approx 0.05$, $a_E \approx 0.01$. Taking these areal densities into account, ρ_{BD} is estimated to be one order of magnitude larger than without consideration of a_i, which is in good agreement with the experimental values. The gray area M_2 in Fig. 3 indicates the possible values for ρ_{BD} in this case. In addition, the ratio $\rho_{BD}(40\text{ K})/\rho_{BD}(20\text{ K})$ is equal to approximately 5, while the theoretical estimation gives a value between 3 and 10. According to Eq. (9), the ratio $\rho_{BD}(40\text{ K})/\rho_{BD}(20\text{ K})$ does not contain the geometry- and diffusion-dependent terms (except for γ_{DC} and γ_{BC} in the brackets) and consequently depends mainly on τ_+ and τ_-, i.e., on temperature.

Our results lead to the conclusion that the geometry of the growth islands can considerably enhance (and in a different configuration of course also attenuate) the anti-Stokes luminescence. The obvious explanation for this is that the areal densities are responsible for the enhancement. However, in the framework of our simple model, the influence of γ_i cannot be estimated. They will also modify the PL properties. If, e.g., the diffusion length is smaller than the characteristic dimension of the islands, then no relaxation or activation processes are possible. Therefore, further analysis of Stokes

and anti-Stokes luminescence in such samples could also provide information on their geometrical properties.

Summarizing, we have observed significant anti-Stokes luminescence at temperatures as low as 20 K in a 5.5 nm wide GaAs/$Al_{0.17}Ga_{0.83}As$ QW with atomically flat growth islands as a result of thermal activation of excitons and their transfer to islands with energetically higher states. Due to geometrical properties of the growth islands, the intensity ratio of anti-Stokes and Stokes luminescence can be enhanced by almost one order of magnitude.

[1] K. Fujiwara, H. Katahama, K. Kanamoto, R. Cingolani, and K. Ploog, Phys. Rev. B **43**, 13 978 (1991).

[2] M. V. Marquezini, M. J. S. P. Brasil, J. A. Brum, P. Poole, S. Charbonneau, and M. C. Tamargo, Phys. Rev. B **53**, 16 524 (1996).

[3] M. Kohl, D. Heitmann, S. Tarucha, K. Leo, and K. Ploog, Phys. Rev. B **39**, 7736 (1989).

[4] K. Fujiwara, K. Kanamoto, and N. Tsukada, Phys. Rev. B **40**, 9698 (1989).

[5] R. Eccleston, R. Strobel, W. W. Rühle, J. Kuhl, B. F. Feuerbacher, and K. Ploog, Phys. Rev. B **44**, 1395 (1991).

[6] E. J. Johnson, J. Kafalas, R. W. Davies, and W. A. Dyes, Appl. Phys. Lett. **40**, 993 (1982).

[7] Y. Mori, K. Onozawa, H. Ohkura, and Y. Chiba, J. Lumin, **48&49**, 800 (1991).

[8] R. Hellmann, A. Euteneuer, S. G. Hense, J. Feldmann, P. Thomas, E. O. Göbel, D. R. Yakovlev, A. Waag, and G. Landwehr, Phys. Rev. B **51**, 18 053 (1995), and references therein.

[9] D. S. Kim *et al.*, Prog. Cryst. Growth Charact. **33**, 161 (1996).

[10] B. M. Ashkinadze, E. Cohen, Arza Ron, and L. Pfeiffer, Phys. Rev. B **47**, 10 613 (1993).

[11] L. Schrottke, H. T. Grahn, and K. Fujiwara, Phys. Rev. B **56**, 13 321 (1997).

[12] G. P. Srivastava, *The Physics of Phonons* (Adam Hilger, Bristol, 1990), pp. 278–283.